Pacific Graphics 2020
E. Eisemann, A. Jacobson, and F.-L Zhang
(Guest Editors)

Volume 39 (2020), Number 7

Visual Analytics in Dental Aesthetics

Aleksandr Amirkhanov,[1] Matthias Bernhard,[2] Alexey Karimov,[2] Sabine Stiller,[2] Andreas Geier,[3] M. Eduard Gröller,[1,4] Gabriel Mistelbauer[5]

[1]TU Wien, Austria [2]cool IT GmbH, Austria [3]Denttec KG, Italy [4]VRVis Research Center, Austria [5]Otto-von-Guericke University Magdeburg, Germany

Abstract

Dental healthcare increasingly employs computer-aided design software, to provide patients with high-quality dental prosthetic devices. In modern dental reconstruction, dental technicians address the unique anatomy of each patient individually, by capturing the dental impression and measuring the mandibular movements. Subsequently, dental technicians design a custom denture that fits the patient from a functional point of view. The current workflow does not include a systematic analysis of aesthetics, and dental technicians rely only on an aesthetically pleasing mock-up that they discuss with the patient, and on their experience. Therefore, the final denture aesthetics remain unknown until the dental technicians incorporate the denture into the patient. In this work, we present a solution that integrates aesthetics analysis into the functional workflow of dental technicians. Our solution uses a video recording of the patient, to preview the denture design at any stage of the denture design process. We present a teeth pose estimation technique that enables denture preview and a set of linked visualizations that support dental technicians in the aesthetic design of dentures. These visualizations assist dental technicians in choosing the most aesthetically fitting preset from a library of dentures, in identifying the suitable denture size, and in adjusting the denture position. We demonstrate the utility of our system with four use cases, explored by a dental technician. Also, we performed a quantitative evaluation for teeth pose estimation, and an informal usability evaluation, with positive outcomes concerning the integration of aesthetics analysis into the functional workflow.

CCS Concepts

• ***Applied computing*** → ***Life and medical sciences;*** • ***Human-centered computing*** → ***Visualization application domains;***

1. Introduction

Oral diseases affect nearly 3.5 billion people worldwide and pose a major health burden for many countries [Wor]. Only 41% of Europeans have all their natural teeth, and a third of the rest wears partial or full, removable dentures [Dir10]. In this paper, we focus on full denture reconstructions. Wearing dentures often brings various difficulties to their owners, such as day-to-day pain or embarrassment. This leads to significant discomfort or other severe consequences, such as long-term social distancing. Furthermore, dental healthcare is expensive and there is a strong correlation between access to dental care and satisfaction with dentures [Wor, Dir10]. Therefore, cost-efficient and accessible solutions are required.

Dental healthcare increasingly employs digital technologies to design and manufacture high-quality and cost-efficient dental prosthetic devices. The modern dental reconstruction workflow (see Figure 1) requires two appointments with the patient [Mer, SKS*17]. During the *first appointment*, a dental technician captures the dental impression of the patient (see Figure 1 a). The impression is a negative imprint of hard and soft mouth tissues, i.e., the residual teeth, and gingiva. Impressions can be obtained traditionally, using a dental tray and a special thermoplastic impression material, or digitally, using an intraoral scanner [MGLL17]. An accurate impression is the foundation for a patient-specific denture. Once the dental impression is acquired, dental technicians use dedicated CAD software to extract several important features from it. First, they determine the *occlusal plane* that covers the incisal edges of the anterior teeth, and the *occlusal surfaces* of the posterior teeth. Second, they remove the jaw undercuts from the impression mesh to ensure a comfortable denture insertion and removal. Next, the denture border lines are drawn on the impression to outline the extents of the denture (see Figure 1 b).

One way to design a full denture starts with the selection of a suitable denture model from a preset, referred to as the *teethmaster*. This is based on the previously extracted features and the aesthetic preferences of the patient. The selection is done from a representative range of teethmasters, based on criteria, such as configuration (one or two molars), bow size (shape of the alveolar line), and the teethmaster functionality concerning statics. Further refinements are made with specific CAD tools that adjust the shape or position of the teeth, to satisfy functional and aesthetic criteria. Then, a prosthesis is generated by modeling the gingiva, which is the interface between the teeth and the denture base. The denture base is derived from a patch, cut from the impression scan with the denture border line, and, thus, fits the jaw of the patient. Fine-grained refinements are made by editing the gingiva to convey a natural appearance (see Figure 1 c).

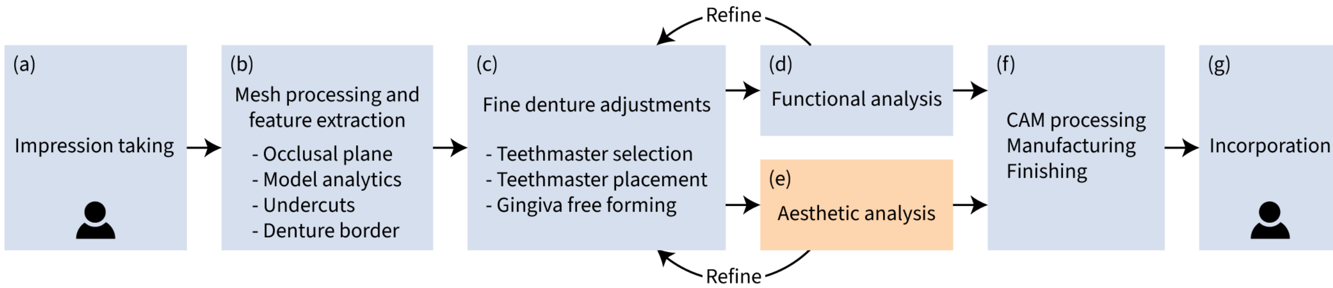

Figure 1: *The modern workflow of dental technicians, as described in Section 1. For the first time, we integrate interactive aesthetics analysis into the workflow, enabling dental technicians to assess functional changes of the denture shape from an aesthetic point of view.*

Additionally, the digital workflow allows specialists to conveniently analyze the functionality of designed dentures for the entire jaw of the patient (see Figure 1 d). With a *virtual articulator*, mandibular movements can be simulated on a digitalized physical model of the mandibular joints and the masticatory apparatus. During the *functional analysis*, issues related to the denture design, such as teeth collisions, are identified and corrected by changing the teeth shape, and the layout or the position of the teeth. Besides having well functioning and comfortably fitting dentures, patients are also interested in aesthetically pleasing denture designs, which greatly affect their overall appearance. Designing a denture that adheres to the aesthetic requests of the patient is a challenging task (see Figure 1 e), which is currently accommodated through the use of the aforementioned teethmasters. Finally, the prosthesis is manufactured utilizing CAM technology (see Figure 1 f). Depending on the used materials, dental technicians may apply various finishing procedures, such as sanding or polishing. Fine denture adjustments are performed during the *second appointment*, when the prosthesis is delivered to the patient (see Figure 1 g).

During the design of dentures, dental technicians consider various facial and dental features for a functional, as well as natural-looking and aesthetic, result. While functional analysis is based on objective criteria, design decisions that concern aesthetics are rather subjective, and rely on the intuition and experience of the dental technician. We contribute to the denture design process with a variety of aesthetic criteria (e.g., proportions) and measurement strategies (e.g., smile lines analysis), implemented as computational tools, and integrated into a denture CAD software. To this end, aesthetic features have to be extracted from the predicted appearance of a patient with new dentures, quantified, and visually conveyed.

In this work, we base our approach upon *predicting* the appearance of a patient with in-line designed dentures, *quantifying* several aspects of dental aesthetics, *visualizing* these aspects interactively during denture design, and *comparing* them. Our approach is integrated into the state-of-the-art digital workflow of dental technicians.

2. Task Analysis

At an early stage of our work, we conducted an informal interview with our collaborating dental technicians. During the interview, we identified two *tasks* (*T1*, *T2*) that should be addressed to improve the current dental workflow concerning the aesthetics analysis of dentures. Every task corresponds to a specific step in the workflow and contains a list of *requirements* (*R 1–R 11*), as summarized below:

T 1 Denture Aesthetics Overview and Assessment: the dental technician selects the most suitable teethmaster for the patient from a large library.

- **R 1** Provide a preview of the dental treatment outcome.
- **R 2** Compare different dentures and assess each case.
- **R 3** Provide an overall score for each denture to quickly identify and compare suitable dentures.
- **R 4** Propose a visualization to identify and show the main problem of each denture.
- **R 5** Propose a visualization to show the golden proportions for the upper teeth.

T 2 Fine Adjustment of Selected Teethmaster: the dental technician adapts the selected teethmaster to the unique jaw anatomy of the patient, and improves it aesthetically.

- **R 6** Provide interactive feedback on all denture adjustments.
- **R 7** Propose a visualization that includes facial proportions.
- **R 8** Propose a visualization to show the six smile lines.
- **R 9** Propose a visualization that includes the three different scales of golden proportions, i.e., the eye scale, mouth scale, and teeth scale.
- **R 10** Provide specific feedback helping to identify, and localize what is the major problem with the denture, and how to correct it.
- **R 11** Integrate the entire solution into the current workflow of dental technicians.

3. Related Work

Our work concerns various topics from visual computing, visualization of the predicted outcome, visual analytics for treatment planning, and facial and dental aesthetics. In this section, we summarize the related work of these topics.

Teeth Pose Estimation: Aichert et al. [AWL*12] presented a method for image-based teeth tracking in a video. They used computed-tomography scans of the jaw of the patient to estimate the position of the maxilla and mandible. Initially, the teeth must be placed manually. Wang et al. [WSH*14] discussed a similar approach to track teeth in a stereo video for augmented reality navigation in maxillofacial surgery. Later, they also introduced a method for a single-camera setup [WSY*17] for oral and maxillofacial surgery. Yang et al. [YMS*19] developed a jaw kinematics model from a stereo video. They used intra-oral scans to track the maxilla and mandible pose. The aforementioned approaches require that a significant part of the teeth is visible and they address different applications. Zoss et al. [ZBGB19] track the jaw movements, based solely on the visible skin surface. Their approach requires training data and may provide inaccurate results if the patient has unique jaw movements, which cannot be triangulated inside the convex hull of the training set.

Predicted Outcome: Zachow et al. [ZHD06] assessed different therapeutic strategies of craniomaxillofacial surgery. In this work, they used tomography images of patients and a finite-element method on various scenarios of treatment outcomes. Lee et al. [TCH01] developed a 3D surgical simulation system for rhinoplasty planning. They use a 3D feature-based volume morphing technique to preview various treatment scenarios. Kim et al. [KLK08] proposed a tool to simulate breast plastic surgery outcomes. With an image-based method, they got a 3D model of the patient and simulated the appearance of the breast of the patient using an example-based algorithm. Keeve et al. [KGPG96] employed a 3D finite element tissue model to predict soft tissue changes from the realignment of underlying bone structures. Chabanas et al. [CLP03] predicted deformations of facial soft tissue from bone repositioning in maxillofacial surgery. The method is based on a generic 3D finite element model and it can provide simulations of face deformations under muscle actions. Gladilin et al. [GZDH04] realistically simulated facial expressions of emotions for craniofacial surgery planning. The aforementioned approaches deal with various applications and cannot be used to predict dental treatment outcomes. Amirkhanov et al. [AAB*18] presented a virtual mirror approach to preview full dentures in augmented reality. Their method estimates the teeth pose based on facial landmarks and replaces natural teeth in a video stream with a denture rendering. The method is limited to provide a preview and cannot be used by dental technicians to assess aesthetic changes caused by fine denture adjustments.

Visual Analytics for Surgery Planning: Krekel et al. [KBV*06] invented a technique for the visualization of a predicted motion range for shoulder replacement. Every change of the treatment planning interactively updates the predicted motion range of the patient, allowing surgeons to identify the most suitable treatment scenario. Dick et al. [DGBW09] presented a stress tensor field visualization of bones for hip joint replacement. The method is interactive and assists surgeons in determining the optimal implant design. Chen et al. [CWP*01] developed a system to assist knee study and operation. The system includes a 3D knee model reconstruction, motion simulation, biomechanical visualization, and virtual surgery. Meehan et al. [MTG03] presented an interactive technique for planning craniofacial surgery. Their method computes non-linear soft-tissue deformations, due to bone realignment. Nadjmi et al. [NMD*10] proposed a semi-automatic method to virtually define the dental occlusion. They use a rigid-motion physical-engine to ensure the impenetrability of dental meshes. All approaches mentioned above are tailored to a specific application and cannot be used for the aesthetics analysis of dentures.

Facial and Dental Aesthetics: The facial attractiveness [TG99, PLPV*98, PBPV*99], as well as smile attractiveness [VdGOVHKJ07,JBS99,HLJ07], were intensively studied in psychology. Recent developments in the machine learning domain also include an automatic facial attractiveness assessment. For example, Eisenthal et al. [EDR06] apply machine learning for computing a facial attractiveness score. Xu et al. [XJL*17] predicted facial beauty from a photo, using a convolutional neural network. Fan et al. [FLL*17] computed facial attractiveness, using a very deep residual network. Liu et al. [LWC*19] presented a tool for face beautification. Their tool manipulates the input face image to increase its aesthetic score. However, most of the work on facial attractiveness assessment and beautification does not consider dental aesthetics.

4. Method

We present a solution for the interactive analysis and exploration of dental aesthetics. To support the aesthetics analysis, we first estimate the teeth pose in the video frame (see Section 4.1). We then extract relevant metrics and visualize them to assist dental technicians in aesthetics analysis of denture and decision making (see Section 4.2). According to *R 11*, the method has been integrated into existing CAD software for designing full dentures from impressions of patients.

4.1. Teeth Pose Estimation

The teeth pose estimation procedure is crucial for the entire aesthetics analysis, as it enables denture preview and aesthetics metric calculation. We estimate the teeth pose in two steps. In the first step, we approximate the teeth pose using only facial landmarks (see Figure 2 a–d). In many cases, this is sufficient to preview the denture. We refer to it as the *approximate teeth pose*. In the second step, we optimize the approximate teeth pose in image space (see Figure 2 e, f) using the dental impression of the patient. We refer to it as the *refined teeth pose*. The refined teeth pose estimation requires that parts of the original teeth of the patient are visible. In cases where only small portions of the original teeth are visible, the refined teeth pose might be inaccurate. To achieve a robust outcome, we compare the refined teeth pose and the approximate teeth pose. If they are dissimilar more than a predetermined threshold, we use the approximate teeth pose for the current frame. If a patient does not have original teeth, it is difficult to create a denture preview because the patient's lips are deformed, especially when smiling. Although a denture preview is possible with the approximate teeth pose, the lip deformation changes the shape of the smile and thus, leads to inaccurate results. In such a case, we suggest using a temporary denture for the patient during the video recording. This temporary denture restores the shape of the lips and can be also used for the refined teeth pose estimation.

4.1.1. Approximation

Following our previous work [AAB*18], we compute an approximate teeth pose by solving a 3D-to-2D point correspondence between the facial landmarks and the 3D face model. We use the maxilla and mandible meshes from the BodyParts3D database [MFT*09] to create the respective models. The maxilla model contains points located on the upper part of the face (see red points in Figure 2 c)

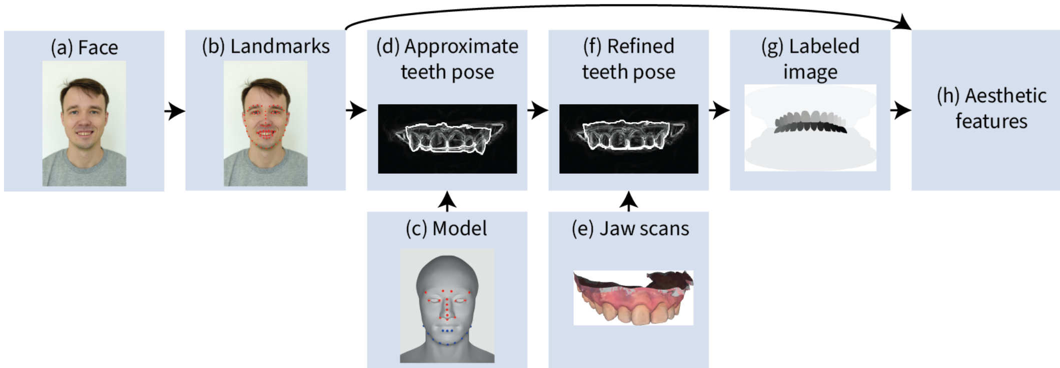

Figure 2: *Metric extraction starts with face detection and landmark extraction. Later, we approximate the teeth pose by solving a 3D-to-2D point correspondence between the head model and facial landmarks. We refine the teeth pose using the impression of the patient. Denture previews are generated by replacing the natural teeth with denture renderings, and we extract aesthetic features from these images.*

Similarly, the mandible model contains points located on the lower lip and the chin (see blue points in Figure 2 c). For every video frame, we detect the face region and extract the facial landmarks (see Figure 2 b) using the Dlib library [Kin09]. These landmarks correspond to the points placed on the maxilla and mandible models. We solve the 3D-to-2D point correspondence using Levenberg-Marquardt optimization [Lev44]—first, for the maxilla (see Figure 2 d). For the mandible, we follow the same procedure as for the maxilla, but we use the earlier detected maxilla pose as a starting configuration. This improves the accuracy of the estimation, as the mandible model contains fewer feature points and is more difficult to detect, compared to the maxilla.

4.1.2. Refinement

We refine the approximate maxilla pose in image space, using the jaw impression of the patient (see Figure 2 e). To measure how well the estimated teeth position matches the actual teeth position, we compute the following features for every video frame: tooth edges, tooth color, and tooth luminance. We define the refinement procedure as an optimization problem with the following optimization function:

$$T = w_e M_e + w_c M_c + w_l M_l, \tag{1}$$

where T is the maxilla pose defined by a 3D position vector, and by three Euler rotation angles; M_e, M_c, M_l are matching metrics for edges, color, and luminance; w_e, w_c, w_l are corresponding weights for the metrics.

To solve Equation 1, we use a pattern search optimization strategy [HJ61] that starts from the initial maxilla pose and refines it by searching a better pose in a neighborhood of the parameters. For the current pose and all candidates, we iteratively compute the function value. If we find a better placement, we use this as the initial pose for the next iteration. Otherwise, we increase the radius of the investigated parameter neighborhood and repeat the search process. If the neighborhood has reached the maximal radius, we stop and consider the currently best pose as the optimum.

Edge Matching: We perform edge matching in the gradient image space. Firstly, we apply Sobel edge detection [KVB88] with the same parameters on both images, i.e., the denture image and the natural teeth image are filtered with the same kernel. Secondly, we remove all non-dental edges like the lips, and face skin irregularities, using the facial landmarks. This avoids solutions of the optimizer, where the dental objects snap to non-dental objects. Thirdly, we multiply the source and destination image edges to see how well the edges for the source and destination images are matching:

$$M_e = \sum_{x=0}^{W-1} \sum_{y=0}^{H-1} I_s(x,y) I_d(x,y), \tag{2}$$

where W is the image width, H is the image height, I_s is the intensity of the source image, and I_d is the intensity of the destination image.

Color Matching: We convert the source image from *RGB* to the *Lab* color space, which consists of three channels: lightness, green-red, and blue-yellow. We use the *Lab* color space, because this color representation is convenient to separate teeth pixels from surrounding pixels belonging to lips, gingiva, and tongue. Moreover, the teeth are well distinguishable from the lips in the green-red channel. We calculate the color matching using the following equation:

$$M_c = \frac{w_a \sigma_a + w_b \sigma_b}{I_{max}}, \tag{3}$$

where σ_a is the standard deviation of the green-red channel, σ_b is the standard deviation of the blue-yellow channel, w_a, w_b are the corresponding weights, and I_{max} is the maximal intensity value.

Luminance Matching: Teeth are typically brighter than their surrounding area and thus can be well differentiated in the lightness channel. We compute the luminance matching as follows:

$$M_l = \frac{\mu}{I_{max}}, \tag{4}$$

where μ is the mean intensity value of all pixels belonging to teeth, and I_{max} is the maximal intensity value.

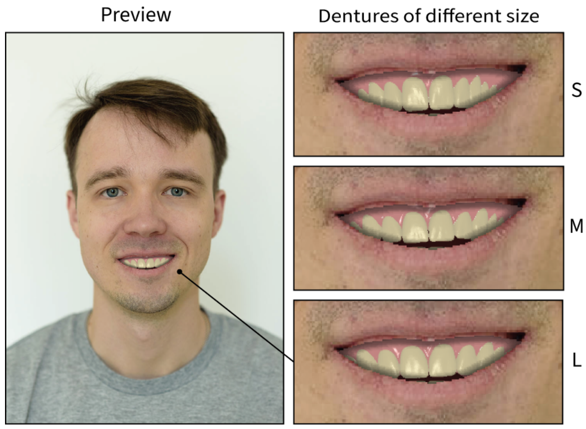

Figure 3: *The denture preview shows the face of the patient, augmented with a denture. The denture can be changed or adjusted during the aesthetics analysis. On the right-hand side, there are three dentures of different size: small (S), medium (M), and large (L).*

4.2. Aesthetics Analysis

Designing dentures requires knowledge and, especially, experience. Considering the user tasks and literature in cosmetic dentistry, we propose a solution for the aesthetics analysis of dentures. This solution enables dental technicians to assess denture aesthetics and to identify and correct possible design flaws. During dental design, technicians often concentrate on a small part, e.g., a single tooth, and forget to consider the overall dental aesthetics. Our approach solves this issue by tracking several states of the denture and visualizing them on demand, to inspect how these changes affect the aesthetics. Additionally, our method computes metrics for aesthetics in the image space for the current denture design. With our aesthetics analysis method, dental technicians can perform fine denture adjustments, i.e., they can transform and rotate every individual tooth. Together with the tooth manipulation, we deform the gingiva with interactive Laplacian mesh editing [SCOL*04] to match the new teeth layout. The control vertices are those which are inside the teeth meshes. Their position is kept fixed relative to the respective reference tooth which contains them. The deformation's region-of-interest is obtained by applying a dilation on all control vertices with a distance of 5 mm. Interactive refresh rates are achieved by splitting the Laplacian solving into a pre-computed factorization pass and an update pass. Also, immediately after the manipulation of the denture, we recompute all metrics in real-time, providing responsive feedback. This addresses *R 6*.

4.2.1. Denture Preview

In the denture preview, we augment the video of the patient with the current denture model. We identify the mouth region from the landmarks and find the upper and lower lip smile lines. Using these lines, we mask out the mouth region in the video frame with a dark red color that mimics the color of the tongue and gingiva. We compute the teeth pose and apply the rotation matrix and the translation vector to the denture model. Then, we render the denture model and combine the rendered image with the video frame. Figure 3 shows a denture preview for three dentures of different sizes. The denture preview addresses *R 1*.

Best Viewing Angle: The frontal view of the face is one of the most important views for the aesthetics analysis, as it highlights problems related to the denture placement or the teeth symmetry, for instance. We developed a procedure that searches for the most frontal frame in the video. For each video frame, using the teeth pose, we compute the angle between the view direction of the teeth and the camera. We select the frame with the smallest angle and use it as a suggestion for the aesthetics analysis.

4.2.2. Facial Proportions

Dental technicians use facial proportions to identify the suitable denture size, shape, and position [Lev78]. Figure 4 a–k shows the most important facial lines. Further in the text, we will refer to these lines with the corresponding letter assigned in the aforementioned figure. The ratio of the distance between lines *(b)* and *(d)* and the distance between lines *(d)* and *(e)* (see Figure 4 l, top) should be approximately equal to the ratio of the sum of the widths of the first three teeth (central incisor, lateral incisor, and canine) to the half-width of the mouth (see Figure 4 l, middle). These two ratios should also be approximately equal to the ratio of the width of the central incisor to the width of the lateral incisor (see Figure 4 l, bottom).

We use this facial view to guide the dental technicians during the aesthetics analysis. The facial proportion view augments the denture preview with facial lines (see Figure 10 a–c and Figure 11 a–g). Vertical lines help dental technicians to identify an appropriate denture size, and horizontal lines assist them to define the denture placement. The facial proportion view addresses *R 7*.

4.2.3. Dental Proportions

Teeth proportions are often used in cosmetic dentistry as an aesthetic metric. Often dental technicians use the golden ratio to define natural proportions between teeth [Lom73]. For natural teeth, the ratio of the central incisor width to the lateral incisor width is approximately equal to the golden ratio (see Figure 4 n). Also, the ratio of the lateral incisor width to the canine width and the ratio of the canine width to the first premolar width is approximately equal to the golden ratio. The visible tooth area depends on the angle of view. The visible tooth widths or proportions are, therefore, view-dependent and must be calculated separately for each video frame.

To extract the teeth proportions, we render the denture model into a labeled image (see Figure 2 g). We then use a threshold segmentation to obtain a mask for each tooth and calculate the extents of the region masks. Horizontal extents indicate teeth boundaries, and all together they depict teeth proportions. The dental proportions view augments the video frame with vertical dental lines, and both the face of the patient and the denture are visible (see Figure 10 d). This view highlights the current teeth proportions and allows dental technicians to assess the symmetry and size of the denture during fine-tuning. Because dental technicians can use dental proportions to detect and correct improper denture placement and size, this view meets *R 10*.

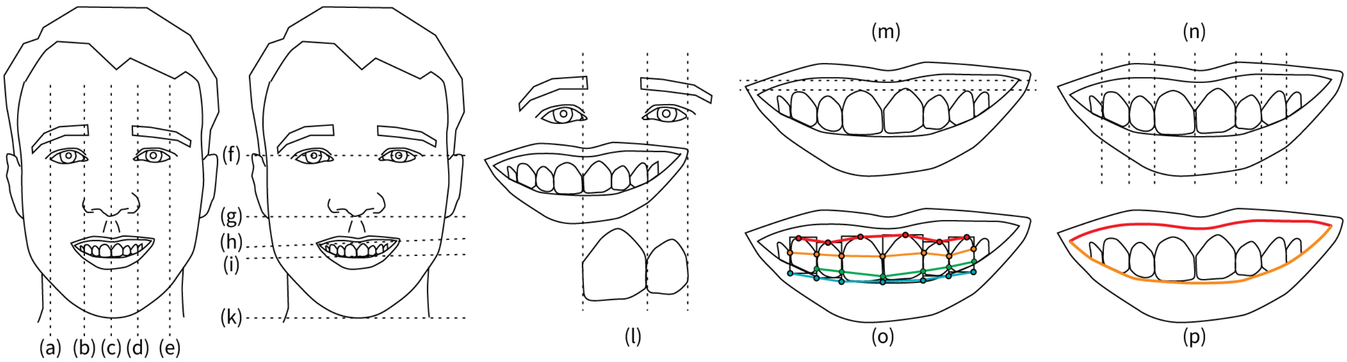

Figure 4: *Facial and dental metrics used in the aesthetics analysis: the two lateral palpebral raphe lines (a), (e), the two intercommissural lines (b), (d), the symmetry line (c), the interpupillary line (f), the acanthion line (g), the intercommissural line (h), the incisor line (i), and the mentum line (k); eyes, mouth, and teeth are in harmony as they have similar internal proportions (l); lip line height (m); proportions between teeth (n); from top to bottom: cervical, papillary, contact points, incisal smile lines (o); upper lip and lower lip smile lines (p).*

4.2.4. Dental Histogram

The amount of visible gingiva has a significant influence on smile aesthetics [dGOHKJ07]. To compute the dental histogram, we identify the mouth region using facial landmarks and render the visible part of the denture behind the lips as the labeled image (see Figure 2 g). Using this labeled image, we segment the gingiva and teeth. Since dental technicians are interested in the horizontal line separating the gingiva from teeth, we compute the number of gingiva and teeth pixels for every row of the image. For every column or row in the image, we compute the number of gingiva pixels and the number of teeth pixels. This provides us with two distributions, which we visualize in the dental histogram (see Figure 11 h, i).

Typically, dental technicians aim to have gingiva with 2–3 mm of visible height [dGOHKJ07]. Based on this histogram, we define the dividing line between the gingiva and teeth at the location where the numbers of gingival and teeth pixels are equal, i.e. where we have an evenly mixed distribution of pixels between the two materials. Since the dental histogram provides a suggestion for the accuracy of the denture placement, it satisfies *R 10*.

4.2.5. Smile Lines

Smile lines are important to quantify dental aesthetics and to identify main flaws in the denture design [Lom73, dGOSKJ11]. They connect features, which are important for the aesthetics analysis of a smile. The line shape provides a visual guideline for the dental technician on smile aesthetics. To address *R 8*, we compute the six aesthetic smile lines presented by Câmara [Câm10]. Figure 4 o–p lists and illustrates these smile lines, and Figure 5 a–d shows these smile lines computed on the face of a person with our method. The *upper-lip smile line* and the *lower-lip smile line* are computed directly from the facial landmarks. The other lines are computed from the labeled image of a denture (see Figure 5 e, f).

Figure 5: *Six aesthetics smile lines. Cervical (a), papillary (b), contact points (c), incisal (d), upper-lip (e), and lower-lip (f) smile lines.*

Cervical Smile Line: The cervical smile line connects the upper corner of the visible parts of the upper teeth. To calculate this line, we extract the tooth contours and search for the point with the lowest value on the Y-axis (vertical axis, pointing downwards) for each tooth. We connect these points to obtain the cervical smile line.

Papillary and Contact Points Smile Lines: The papillary smile line connects the tips of the gingiva between the canines and the lateral incisors, and between the maxillary lateral incisors and the central incisors. To compute the papillary and the contact points smile lines, we apply a dilation operator to the teeth masks and compute their overlapping areas. The kernel of the dilation operator should only modify the object along the X-axis (horizontal axis) to ensure the correct position of the points. After computing the contours of the overlapping regions, we determine the upper and lower contour points. The papillary smile line is defined as the line connecting the upper points, while the contact points line connects the lower points.

Incisal Smile Line: The incisal smile line connects the edges of the anterior maxillary teeth. To compute this line, we extract the teeth masks and calculate the corresponding bounding boxes. From the bounding boxes, we find the lowest edges, and we connect them.

Upper-Lip and Lower-Lip Smile Lines: We compute the upper and lower lip smile lines only from the facial landmarks. Following our previous work [AAB*18], we increase the number of points on the lips.

4.2.6. Harmony View

The face has repetitive proportions at different scales, i.e., the eyes, mouth, and teeth have similar proportions [Lev78] (see Figure 4 l). To evaluate and compare them, we designed the *harmony view*. The harmony view shows the eye, mouth, and teeth subviews, and

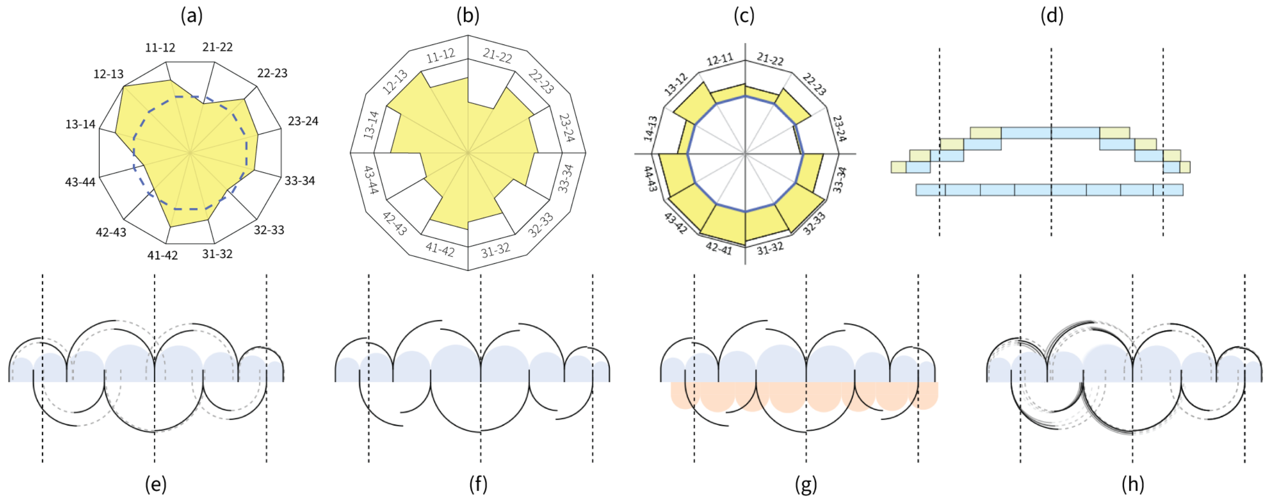

Figure 6: *The evolution of the design of the abstracted facial and dental proportions view in chronological order: the radar visualization (a)–(c), the stairway visualization (d), and the modulor visualization (e)–(h).*

their corresponding internal proportions (see Figure 10 e). Dental technicians can choose one as the reference subview, and we align all other subviews to the reference one. In the subviews, we show the actual proportions as small blue lines and the reference proportion as red lines. Our employed harmony view addresses *R 9*.

4.2.7. Abstracted Facial and Dental Proportions

Dental technicians often use the golden ratio to approximate the desired proportions for the upper teeth [Lev78]. Lower teeth are, in many cases, not visible. Therefore, dental technicians usually adjust them to achieve a good functional state of the denture. Nevertheless, the lower teeth proportions are also important for aesthetics analysis. Together with our collaborators, we designed three visual techniques for abstracted facial and dental proportions—namely, a *radar*, a *stairway*, and a *modulor view*. We compared and assessed these techniques to select the most suitable one for integration in the dental CAD system. This was found to be the modulor, as we discuss below. In this section, we briefly discuss these techniques and our methodology for choosing the final technique.

The **radar** visualization displays the proportions for the upper and lower teeth in a circular layout that mimics the teeth layout (see Figure 6 a–c). Around every bar, we show a label indicating the ratio of the teeth pair that the bar represents. The ratio of a teeth pair is defined as the ratio of the widest to the thinnest tooth and is always between zero and one. The design in Figure 6 a, c includes a blue polygonal line that indicates the golden proportion. The line assists technicians in estimating how much the actual proportion deviates from the desired one. The advantage of the *radar* visualization is an intuitive and clean representation of teeth proportions that allows technicians to compare various dentures in a short time. The main disadvantage of the *radar* visualization is that it includes only dental proportions but no facial ones.

The **stairway** visualization depicts the proportions for the upper and lower teeth with horizontal bars. It also includes three facial lines—the *symmetry line*, the *left eye line*, and the *right eye line*. Figure 6 d shows an example of the stairway visualization. Every bar consists of two rectangles and represents a proportion of the upper teeth pairs. The blue rectangle shows the actual tooth width and the yellow rectangle shows the required width of the next tooth so that both are in perfect proportion to each other, e.g., in the golden ratio. We shift the upper teeth bars down for the next teeth pairs to avoid overlaps. At the bottom, we show the proportions for the lower teeth, which consist only of blue rectangles representing the actual teeth widths. The advantage of the *stairway visualization* is that it shows dental as well as facial proportions. However, it shows the estimated perfect proportion only in one direction, e.g., for the lateral incisor it shows only the canine tooth, but not the central incisor proportion. We can resolve this by displaying yellow bars on both the left and right sides. In some cases, however, this leads to overlapping bars. In an informal interview with our collaborating dental technician, we noticed that the visualization is less intuitive than, for instance, the *radar* visualization, and typically requires a steeper learning curve for an inexperienced dental technician.

The **modulor** visualization encodes the teeth in glyphs and the teeth proportions in arcs (see Figure 6 e–h). Every ratio of a tooth pair has two arcs. For example, the left central incisor and the left lateral incisor are typically in the golden proportion. If they are not in the golden or required proportion, this can be interpreted in two ways, depending on which tooth is considered to be the reference. If the lateral incisor is the reference then the central incisor is too wide. If the central incisor is the reference then the lateral incisor is too narrow. To accommodate this ambiguity in the modulor visualization, we show the ratio between two teeth as two arcs. One arc takes the size of the first tooth as the reference, while the other arc takes the size of the second tooth as the reference. If the teeth are in perfect proportion to each other, these two arcs fit together and look like one continuous arc, without any interruption. Otherwise, the distance between the two arcs indicates the extent of the ratio violation and the direction in which the adjustment

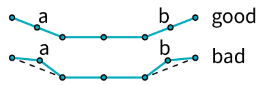

Figure 7: *The incisal smile line shape affects the smile score. The upper and lower rows show a good and bad incisal smile line shape, respectively.*

must be made to improve the denture aesthetics. The design of the visualization was inspired by the work of Le Corbusier, the Modulor [Cor82]. The advantage of modulor is that it shows all dental and facial proportions, as well as bi-directional proportions, and it provides an easier and cleaner reading of the proportions.

In all three presented visualizations, we depict previous dental states as visual trails (see Figure 6 h for the modulor). This allows dental technicians to perform fine denture adjustments while focusing on the denture itself, and then assess how additional changes affected tooth proportions and smile aesthetics. Abstracted facial and dental proportions enable the assessment and comparison of different dentures (*R 2*). They can be used to identify main dental issues, e.g., asymmetric dental layout (*R 4*). Additionally, they show golden proportions for the upper teeth (*R 5*).

4.2.8. Aesthetometer

Using the extracted facial and dental features, we calculate the *total smile score*. Since smile aesthetics are subjective and may vary depending on many different parameters, this *score* is also subjective. However, in case of subtle differences, this score is particularly useful for quantitatively comparing two denture designs. The total smile score consists of scores of three different scores, and is computed according to the formula:

$$S = S_t + S_l + S_i, \tag{5}$$

where S_t is the teeth proportion score, S_l is the symmetry score of the aesthetic lines, and S_i is the incisal smile line score.

The teeth proportion score reflects how well the current teeth proportions match the reference proportions. We calculate this score by the following formula:

$$S_t = \sum_{i=1}^{N} w|r_i - r_{i,d}|, \tag{6}$$

where N is the number of teeth ratios, w is a user-defined weight, r_i is the i-th ratio, and $r_{i,d}$ is the desired ratio for the i-th pair of teeth.

Since all aesthetic lines must be symmetric in the frontal view, we use symmetry to highlight good denture designs. We compute the symmetry score as following:

$$S_l = \sum_{i=1}^{6} \frac{\sum_{j=1}^{\lfloor L_i/2 \rfloor} |p_{i,j} - p_{i,L_i+1-j}|}{D_i}, \tag{7}$$

where L_i is the number of points on i-th line, $p_{i,j}$ is the j-th point of i-th line, p_{i,L_i+1-j} is the antagonist point of j-th point of i-th line, D_i is the length of i-th line.

We compute the incisal smile line score, as following:

$$S_i = 1 - \frac{w}{D}\left(|a - a_{best}| + |b - b_{best}|\right), \tag{8}$$

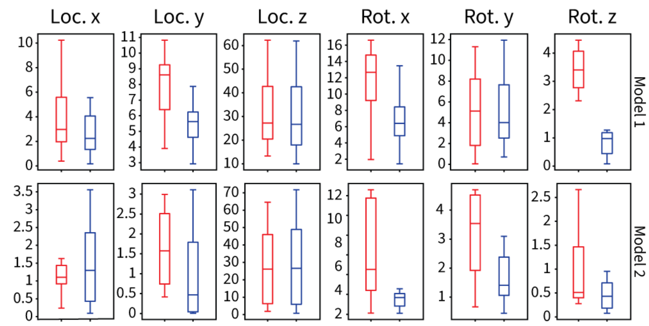

Figure 8: *The upper and lower rows show the error for the first and the second gold standard models, respectively. Box plots depict the mean value and the distribution of the error for the approximate teeth pose estimation (blue), and the refined teeth pose estimation (red) in six dimensions (X, Y, Z coordinates and X, Y, Z Euler rotation angles). The coordinates are measured in millimeters, and the angles are measured in degrees.*

where w is a user-defined weight, a is the left evaluated point of the incisal smile line, a_{best} is the best location of the left evaluated point, b is the right evaluated point of the incisal smile line, and b_{best} is the best location of the right evaluated point (see Figure 7), and D is the length of the incisal smile line.

We visualize the smile score in the aesthetometer, using a gauge visual metaphor. The aesthetometer looks like, e.g., a car speedometer or a pressure gauge (see Figure 12 c, g). If the score is high, the arrow points towards the right. If the score is low, the arrow points to the left. At the bottom of the aesthetometer, we display the numerical value of the smile score. To track changes of the gauge, we display previous values as trails that fade over time. A similar trail concept for gauge widgets was presented by Matkovic et al. [MHSG02]. The aesthetometer addresses *R 3*.

5. Results and Evaluation

After designing the system, we performed a quantitative evaluation of the teeth pose estimation. Besides, we conducted an informal interview with a dental technician. Together with the dental technician, we investigated four use cases to assess various components of the system and to identify how well the proposed solution solves the real-world tasks.

5.1. Teeth Pose Estimation

To evaluate the accuracy and precision of the teeth pose estimation technique, we acquired gold standard data using photogrammetry. We reconstructed two textured face models of a person from a set of high-resolution photographs, but with different facial expressions. Using a single full-frame DSLR camera, we took 19 and 25 photos of the person's face from different angles, for the first and second models respectively. To minimize facial motion between photos, we did the entire procedure in a short time frame (6 and 4 seconds, respectively). We subsequently manually aligned the scanned teeth model of the same person with the head model so that the

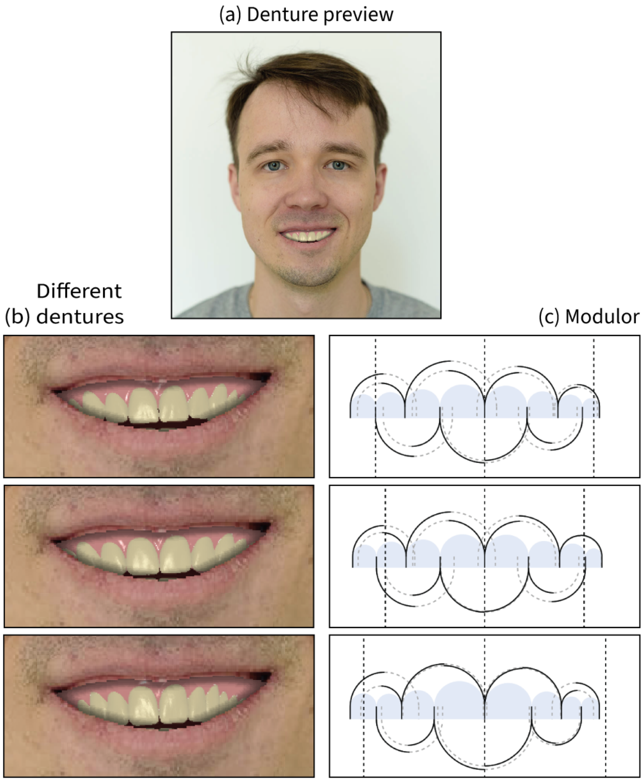

Figure 9: *Comparison and assessment of different teethmasters conducted in Use Case A (Sect. 5.2) with the aid of the denture preview (a)–(b), and the modulor view (c).*

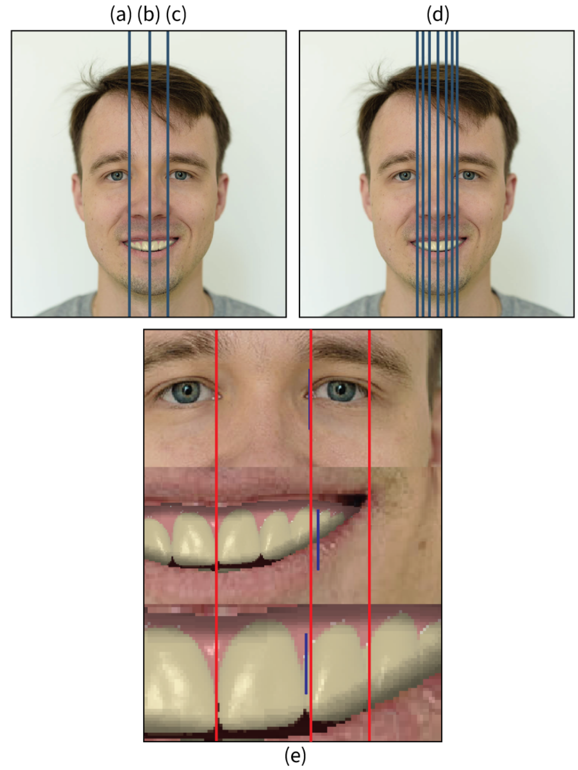

Figure 10: *Analysis of the denture size conducted in Use Case B (see Section 5.2), using the facial proportions view (a)–(c), the dental proportions view (d), and the harmony view (e).*

teeth model matched the contours of the teeth that were visible on the texture of the head model. Then, we rendered each head model with the visible natural teeth from different view positions and directions, defined by the matrix transformations $m_1, \ldots, m_n$. Consequently, we obtained $n = 30$ and $n = 12$ images that look similar to the original photos and were used as input for both teeth pose estimating techniques. For both models, we compared both the approximated and the refined teeth pose against the gold standard, i.e., the position of the aligned teeth model with the additional transformations $m_1, \ldots, m_n$. Figure 8 shows the mean error and the error distribution of both teeth pose estimation techniques (approximated and refined) in all six dimensions (3D location vector and 3D rotation vector) for the two head models. The overall accuracy of the presented imaged-based teeth pose estimation (refined) is higher than that of the landmark-based teeth pose estimation (approximate).

5.2. Use Cases

Use Case A—Choosing the Best Aesthetically Fitting Denture: Our collaborating dental technician has a large library of teethmasters among which he wants to identify the one that best fits the patient. He receives a prerecorded video of the patient, consisting of 340 frames, and he uses the denture preview (see Figure 9 a) to assess the aesthetics of the individual dentures. He goes through the video to preview the overall denture fitting. Later, he identifies a suitable frame for the aesthetics analysis and the comparison of dentures using the best viewing angle identification procedure. As the direct visual comparison might be challenging, he enables the modulor view (see Figure 9 c) to analyze the facial and dental proportions. Afterward, he switches to a different teethmaster (see Figure 9 b), and receives the updated denture preview, as well as the modulor view. Based on the facial shape and the denture proportions, the dental technician compares and assesses all available teethmasters to decide which one fits best for the patient. In this case, the modulor shows the smallest overall discrepancies for the third denture (see Figure 9 c, bottom). This is the best fitting denture, concerning the frontal teeth.

Use Case B—Finding the Suitable Denture Size: The size of the denture must match the size of the face and the facial proportions of the patient. Using the facial proportions (see Figure 10 a–c) as well as the dental proportions (see Figure 10 d), our collaborating dental technician identifies the correspondence between the denture and the face. If the denture has the proper size, the (b) and (d) lines (see Figure 4) should go through the border between canines and first premolars (see Figure 10 a, c). If the denture is too small or too large, he scales the denture up or down or, in some cases, changes the denture preset. Afterward, he uses the harmony view to crosscheck the proportions at different scales. In the harmony view (see Figure 10 e), he can choose the reference proportions, e.g., the

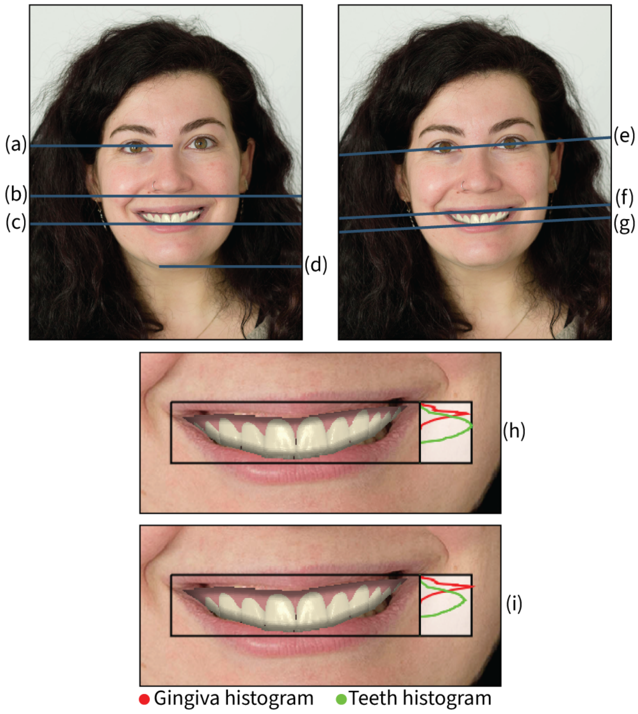

Figure 11: *Analysis of the denture position conducted in Use Case C (see Section 5.2). Facial proportion views (a)–(g) identify the correct denture position. The dental histogram (h)–(i) provides an overview of red-white aesthetics.*

distance between eyes and the eye width. In this case, the selected denture size fits well.

Use Case C—Adjusting the Denture Position: The denture position and orientation play an important role in smile aesthetics. Also, they directly define the size of the visible gingiva surface and the dental surface. Dental technicians employ the term of red-white aesthetics to describe this relationship. Using the facial proportion view, our collaborating dental technician adjusts the vertical denture position. He looks at four horizontal lines, namely lines (f), (g), (i), and (k) (see Figure 4), which should form two golden ratios (see Figure 11 a–d). Besides, he adjusts the denture orientation using lines (f), (h), and (i) (see Figure 4). If lines (i) and (h) are not parallel, the orientation of line (i) must be interpolated between the orientation of line (f) and (h) (see Figure 4). Then, he analyzes the red-white aesthetics in the dental histogram view that shows the distribution of the gingiva and dental pixels in the image. For example, if the number of gingiva pixels is too small (see Figure 11 h), dental technicians can move dentures down to increase their number and reach the target proportion (see Figure 11 i).

Use Case D—Fine Denture Adjustments: During the fine denture adjustments or teeth editing, dental technicians modify the shape of individual teeth and the gingiva to improve the functional aspect of the denture. Our collaborating dental technician uses the virtual articulator to simulate the chewing and biting patterns of the patients and identify functional issues of the teeth, which often result in changing the teeth layout and editing. To preview and assess these changes concerning aesthetics, dental technicians can use a combination of different views. Our collaborating dental technician uses the smile lines view (see Figure 12 a) to get a summary on the current teeth layout, and checks if there are some issues related, for instance, to an asymmetric teeth placement or incorrect smile arc. Using the abstracted facial and dental proportion view (see Figure 12 b), he assesses the dental and facial proportions. If the proportions of teeth are sub-optimal concerning the aesthetics, dental technicians can modify the teeth shape, size, and layout. This view also encodes information about several previous changes as trails, enabling dental technicians to analyze their previous manipulations. If dental technicians are unsure about the current smile aesthetics, they can use the aesthetometer (see Figure 12 c). Using the harmony view, dental technicians see the correspondence of proportions at different scales (see Figure 12 d, h). Every tooth adjustment results in an automatic metric recalculation and update of the views. Figure 12 e–h show updated views, for adjustments in the left frontal incisor and the left canine, from the view of the patient.

5.3. User Experience

To evaluate the user experience, we completed all four usage scenarios together with our collaborating dental technician and asked him to rate the fulfillment of each task requirement regarding *effectiveness* (es), *efficiency* (ey), and *satisfaction* (s). For ranking, we applied a Likert scale from 1 (--) to 5 (++). Requirements related to *T1*—*R1* (es5 ey3 s2), *R2* (es4 ey3 s2), *R3* (es3 ey4 s3), *R4* (es4 ey4 s3), *R5* (es4 ey4 s4)—received positive grades in effectiveness and efficiency. This shows that the proposed solution can be successfully used to achieve the goal in a reasonable amount of time. However, the technician reported that the user interface is overloaded. The technician highly appreciated the different views for abstracted facial and dental proportions and noted that they are understandable and self-explanatory. The requirements of *T2*—*R6* (es4 ey4 s3), *R7* (es4 ey4 s3), *R8* (es4 ey4 s3), *R9* (es3 ey4 s3), *R10* (es4 ey3 s3), *R11* (es3 ey3 s3)—received all positive grades regarding effectiveness, efficiency, and satisfaction. The technician reported that some operations required too many user operations to achieve the goal and some important facial lines were missing. We added these facial lines shortly after the evaluation. The technician appreciated the integration of the aesthetics analysis into the dental CAD workflow. He commented that the aesthetics analysis can be distributed over various steps of the workflow to avoid the cluttered user interface. For example, only some visualizations are necessary for the denture selection step. Besides, we applied the *System Usability Scale* evaluation scheme, which confirmed the previously mentioned observations on the system.

In the open discussion session of the evaluation, we talked about the limitations of the solution and the direction for future work. The main limitation is the complexity of the system and the overloaded user interface. A simpler solution with fewer visualizations should improve the learning curve of the system and facilitate the analysis. Also, smart suggestions about which views are helpful to the current analysis step are important. As future work, we plan to design an additional lateral side view for the aesthetics analysis of the patient. This view can be especially useful for the dental technicians to

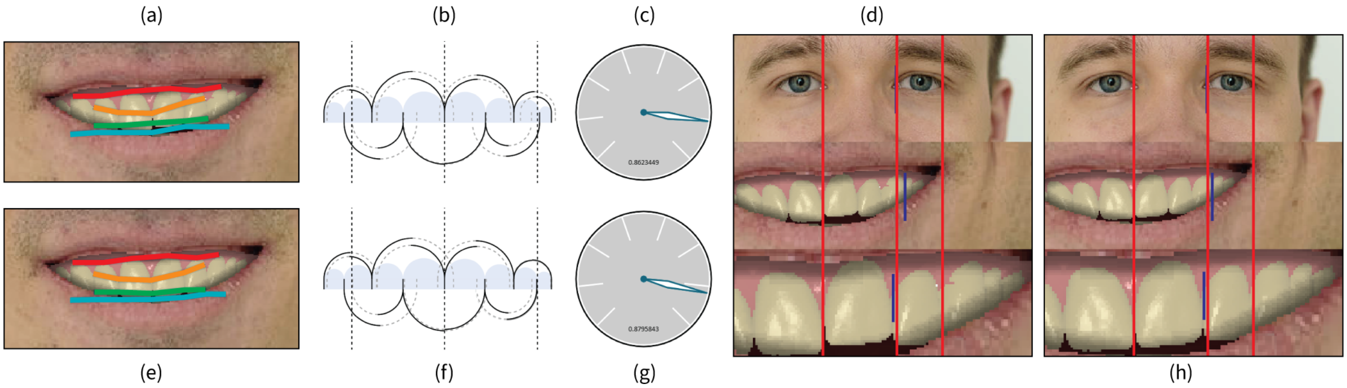

Figure 12: *Analysis of fine denture adjustments conducted in Use Case D (see Section 5.2). The smile lines (a), the modulor (b), the aesthetometer (c), and the harmony view (d) show the current aesthetics state. These views are automatically updated after every tooth editing operation (e)–(h).*

preview the denture placement outcome, as the denture modifies the lip shape. In this view, the shape of the lips must be modified, according to the denture position. Additionally, the fine denture adjustments should be done directly in the abstracted views. This should improve the performance of the designing process as some teeth editing operations require more user interaction. For example, to bring a tooth in front, the camera view must be changed a couple of times.

6. Conclusions and Future Work

The modern dental reconstruction workflow enables the design and manufacturing of high-quality and cost-efficient dentures. For the first time, we integrated an interactive full aesthetics analysis into the current workflow, to provide a functional and aesthetics analysis side-by-side. This combination allows dental technicians to preview the effect of any change in the denture design, both in terms of functionality and aesthetics. In this work, we made the first step towards a systematic smile design by quantifying several aspects of aesthetics, and by visualizing them during the denture design process.

There are several promising directions for future work. Firstly, the proposed method targets dental technicians as prime users of the system. However, including the patient directly in the analysis procedure will increase the confidence and trust of the patient in the treatment outcome. In this case, the system can be used as a platform for communication between patients and technicians. Secondly, the current approach requires a video of the patient to preview the denture. However, additional lateral views can be beneficial for the analysis. Providing a 3D recording of the facial performance of the patient, on one side will increase the complexity of the system; on another side, it will enable additional views, e.g., the side view. Thirdly and finally, enabling the aesthetics analysis for partial dentures, e.g., comprising one tooth or two teeth, is a promising direction. In this case, the dental aesthetics of the patient are constrained not only by the facial features and the jaw anatomy but also by the remaining natural teeth.

Acknowledgment: This work has been financed by the Visual Analytics for Realistic and Aesthetic Smile Design (SmileAnalytics) project, supported by the Austrian Research Promotion Agency (FFG) project no. 861168. VRVis is funded by BMVIT, BMDW, Styria, SFG, and Vienna Business Agency in the scope of COMET—Competence Centers for Excellent Technologies (854174), managed by FFG.

References

[AAB*18] Amirkhanov A., Amirkhanov A., Bernhard M., Toth Z., Stiller S., Geier A., Gröller E., Mistelbauer G.: With-Teeth: Denture Preview in Augmented Reality. In *Vision, Modeling and Visualization* (2018), The Eurographics Association. 3, 6

[AWL*12] Aichert A., Wein W., Ladikos A., Reichl T., Navab N.: Image-based tracking of the teeth for orthodontic augmented reality. In *Medical Image Computing and Computer-Assisted Intervention – MICCAI* (Berlin, Heidelberg, 2012), Springer Berlin Heidelberg, pp. 601–608. 2

[Câm10] Câmara C. A.: Aesthetics in orthodontics: Six horizontal smile lines. *Dental Press Journal of Orthodontics 15*, 1 (2010), 118–131. 6

[CLP03] Chabanas M., Luboz V., Payan Y.: Patient specific finite element model of the face soft tissues for computer-assisted maxillofacial surgery. *Medical Image Analysis 7*, 2 (2003), 131–151. 3

[Cor82] Corbusier F. L.: *Le Corbusier Archive: Le Modulor and other buildings and projects, 1944–1945*. Le Corbusier Archive. Garland Pub., 1982. 8

[CWP*01] Chen J. X., Wechsler H., Pullen J. M., Ying Zhu, MacMahon E. B.: Knee surgery assistance: patient model construction, motion simulation, and biomechanical visualization. *IEEE Transactions on Biomedical Engineering 48*, 9 (2001), 1042–1052. 3

[DGBW09] Dick C., Georgii J., Burgkart R., Westermann R.: Stress tensor field visualization for implant planning in orthopedics. *IEEE Transactions on Visualization and Computer Graphics 15*, 6 (2009), 1399–1406. 3

[dGOHKJ07] der Geld P. V., Oosterveld P., Heck G. V., Kuijpers-Jagtman A. M.: Smile attractiveness. *The Angle Orthodontist 77*, 5 (2007), 759–765. 6

[dGOSKJ11] der Geld P. V., Oosterveld P., Schols J., Kuijpers-Jagtman A. M.: Smile line assessment comparing quantitative measurement and visual estimation. *American Journal of Orthodontics and Dentofacial Orthopedics 139*, 2 (2011), 174–180. 6

[Dir10] DIRECTORATE GENERAL HEALTH AND CONSUMERS: Eurobarometer 72.3: Oral health, 2010. https://ec.europa.eu/commfrontoffice/publicopinion/archives/ebs/ebs_330_en.pdf. Accessed 19.05.2020. 1

[EDR06] EISENTHAL Y., DROR G., RUPPIN E.: Facial attractiveness: Beauty and the machine. *Neural Computation 18*, 1 (2006), 119–142. 3

[FLL*17] FAN Y.-Y., LIU S., LI B., GUO Z., SAMAL A., WAN J., LI S. Z.: Label distribution-based facial attractiveness computation by deep residual learning. *IEEE Transactions on Multimedia 20*, 8 (2017), 2196–2208. 3

[GZDH04] GLADILIN E., ZACHOW S., DEUFLHARD P., HEGE H.-C.: Anatomy-and physics-based facial animation for craniofacial surgery simulations. *Medical and Biological Engineering and Computing 42*, 2 (2004), 167–170. 3

[HJ61] HOOKE R., JEEVES T. A.: "Direct search" solution of numerical and statistical problems. *Journal of the ACM (JACM) 8*, 2 (1961), 212–229. 4

[HLJ07] HÖFEL L., LANGE M., JACOBSEN T.: Beauty and the teeth: perception of tooth color and its influence on the overall judgment of facial attractiveness. *International Journal of Periodontics & Restorative Dentistry 27*, 4 (2007). 3

[JBS99] JOHNSTON C., BURDEN D., STEVENSON M.: The influence of dental to facial midline discrepancies on dental attractiveness ratings. *European Journal of Orthodontics 21*, 5 (1999), 517–522. 3

[KBV*06] KREKEL P. R., BOTHA C. P., VALSTAR E. R., DE BRUIN P. W., ROZING P. M., POST F. H.: Interactive simulation and comparative visualisation of the bone-determined range of motion of the human shoulder. In *SimVis* (2006). 3

[KGPG96] KEEVE E., GIROD S., PFEIFLE P., GIROD B.: Anatomy-based facial tissue modeling using the finite element method. In *Proceedings of Seventh Annual IEEE Visualization* (1996), pp. 21–28. 3

[Kin09] KING D. E.: Dlib-ml: A machine learning toolkit. *Journal of Machine Learning Research 10* (2009), 1755–1758. 4

[KLK08] KIM Y., LEE K., KIM W.: 3d virtual simulator for breast plastic surgery. *Computer Animation and Virtual Worlds 19*, 3-4 (2008), 515–526. 3

[KVB88] KANOPOULOS N., VASANTHAVADA N., BAKER R. L.: Design of an image edge detection filter using the sobel operator. *IEEE Journal of solid-state circuits 23*, 2 (1988), 358–367. 4

[Lev44] LEVENBERG K.: A method for the solution of certain non-linear problems in least squares. *Quarterly of Applied Mathematics 2*, 2 (1944), 164–168. 4

[Lev78] LEVIN E. I.: Dental esthetics and the golden proportion. *The Journal of Prosthetic Dentistry 40*, 3 (1978), 244–252. 5, 6, 7

[Lom73] LOMBARDI R. E.: The principles of visual perception and their clinical application to denture esthetics. *The Journal of Prosthetic Dentistry 29*, 4 (1973), 358–382. 5, 6

[LWC*19] LIU X., WANG R., CHEN C.-F., YIN M., PENG H., NG S., LI X.: Face beautification: Beyond makeup transfer. *arXiv preprint arXiv:1912.03630* (2019). 3

[Mer] MERZ DENTAL GMBH: Baltic denture system. https://www.baltic-denture-system.de. Accessed: 12.06.2020. 1

[MFT*09] MITSUHASHI N., FUJIEDA K., TAMURA T., KAWAMOTO S., TAKAGI T., OKUBO K.: BodyParts3D: 3d structure database for anatomical concepts. *Nucleic Acids Research 37*, suppl 1 (2009), D782–D785. 3

[MGLL17] MANGANO F., GANDOLFI A., LUONGO G., LOGOZZO S.: Intraoral scanners in dentistry: a review of the current literature. *BMC Oral Health 17*, 1 (2017). 1

[MHSG02] MATKOVIC K., HAUSER H., SAINITZER R., GRÖLLER M. E.: Process visualization with levels of detail. In *IEEE Symposium on Information Visualization.* (2002), IEEE, pp. 67–70. 8

[MTG03] MEEHAN M., TESCHNER M., GIROD S.: Three-dimensional simulation and prediction of craniofacial surgery. *Orthodontics & craniofacial research 6* (2003), 102–107. 3

[NMD*10] NADJMI N., MOLLEMANS W., DAELEMANS A., HEMELEN G. V., SCHUTYSER F., BERGÉ S.: Virtual occlusion in planning orthognathic surgical procedures. *International Journal of Oral and Maxillofacial Surgery 39*, 5 (2010), 457–462. 3

[PBPV*99] PERRETT D. I., BURT D. M., PENTON-VOAK I. S., LEE K. J., ROWLAND D. A., EDWARDS R.: Symmetry and human facial attractiveness. *Evolution and human behavior 20*, 5 (1999), 295–307. 3

[PLPV*98] PERRETT D. I., LEE K. J., PENTON-VOAK I., ROWLAND D., YOSHIKAWA S., BURT D. M., HENZI S., CASTLES D. L., AKAMATSU S.: Effects of sexual dimorphism on facial attractiveness. *Nature 394*, 6696 (1998), 884–887. 3

[SCOL*04] SORKINE O., COHEN-OR D., LIPMAN Y., ALEXA M., RÖSSL C., SEIDEL H.-P.: Laplacian Surface Editing. In *Symposium on Geometry Processing* (2004), The Eurographics Association. 5

[SKS*17] STEINMASSL P.-A., KLAUNZER F., STEINMASSL O., DUMFAHRT H., GRUNERT I.: Evaluation of currently available cad/cam denture systems. *Int J Prosthodont 30*, 2 (2017), 116–22. 1

[TCH01] TONG-YEE LEE, CHAO-HUNG LIN, HAN-YING LIN: Computer-aided prototype system for nose surgery. *IEEE Transactions on Information Technology in Biomedicine 5*, 4 (2001), 271–278. 3

[TG99] THORNHILL R., GANGESTAD S. W.: Facial attractiveness. *Trends in Cognitive Sciences 3*, 12 (1999), 452–460. 3

[VdGOVHKJ07] VAN DER GELD P., OOSTERVELD P., VAN HECK G., KUIJPERS-JAGTMAN A. M.: Smile attractiveness: self-perception and influence on personality. *The Angle Orthodontist 77*, 5 (2007), 759–765. 3

[Wor] WORLD HEALTH ORGANIZATION: Oral health: Key facts. https://www.who.int/news-room/fact-sheets/detail/oral-health. Accessed: 19.05.2020. 1

[WSH*14] WANG J., SUENAGA H., HOSHI K., YANG L., KOBAYASHI E., SAKUMA I., LIAO H.: Augmented reality navigation with automatic marker-free image registration using 3-d image overlay for dental surgery. *IEEE Transactions on Biomedical Engineering 61*, 4 (2014), 1295–1304. 2

[WSY*17] WANG J., SUENAGA H., YANG L., KOBAYASHI E., SAKUMA I.: Video see-through augmented reality for oral and maxillofacial surgery. *The International Journal of Medical Robotics and Computer Assisted Surgery 13*, 2 (2017), e1754. 3

[XJL*17] XU J., JIN L., LIANG L., FENG Z., XIE D., MAO H.: Facial attractiveness prediction using psychologically inspired convolutional neural network (pi-cnn). In *2017 IEEE International Conference on Acoustics, Speech and Signal Processing (ICASSP)* (2017), IEEE, pp. 1657–1661. 3

[YMS*19] YANG W., MARSHAK N., SÝKORA D., RAMALINGAM S., KAVAN L.: Building anatomically realistic jaw kinematics model from data. *The Visual Computer 35*, 6-8 (2019), 1105–1118. 3

[ZBGB19] ZOSS G., BEELER T., GROSS M., BRADLEY D.: Accurate markerless jaw tracking for facial performance capture. *ACM Transactions on Graphics 38*, 4 (2019), 1–8. 3

[ZHD06] ZACHOW S., HEGE H.-C., DEUFLHARD P.: Computer assisted planning in cranio-maxillofacial surgery. *CIT 14* (2006), 53–64. 3